Indian Journal of Pure & Applied Physics
Vol. 58, April 2020, pp. 213-217

Specific absorbed fraction of energy of silicon-boron alloys

KV Sathish[a], H C Manjunatha[a*], L Seenappa[a], K N Sridhar[b], N Nagaraj[b] & S Alfred Cecil Raj[c]

[a]Department of Physics, Government College for Women, Kolar 563 101, India

[b]Department of Physics, Government First Grade College, Kolar 563 101, India

[c]Department of Physics, St. Joseph's College, Trichy 620 020, India

Received 17 February 2020

We have studied the energy absorption buildup factors and specific absorbed fraction of energy for the silicon-boron alloys of different composition such as alloy A-$Si_{0.95}$-$B_{0.05}$, alloy B- $Si_{0.9}$-$B_{0.1}$, alloy C- $Si_{0.8}$-$B_{0.2}$, alloy D- $Si_{0.7}$-$B_{0.3}$, alloy E- $Si_{0.6}$-$B_{0.4}$ and alloy F- $Si_{0.5}$-$B_{0.5.}$ for wide energy range (0.015–15 MeV) up to the penetration depth of 40 mfp using geometric progression fitting method. Buildup factors increase with the increase in the penetration depth. It has been found that the shielding parameters such as mass attenuation coefficient, effective atomic number and buildup factor values are larger for the silicon-boron alloy $Si_{0.95}$-$B_{0.05}$ than the other studied silicon-boron alloys. Specific absorbed fraction of energy is maximum for the silicon-boron alloy $Si_{0.95}$-$B_{0.05.}$ Hence, we can conclude that the silicon-boron alloy $Si_{0.95}$-$B_{0.05}$ is a good absorber of X-rays, gamma and neutrons among the studied alloys. The present study is useful in the field of radiation shielding.

Keywords: Energy absorption, Buildup factor, Silicon-boron alloys, Radiation shielding

1 Introduction

When gamma and X-rays enter the medium, they degrade their energy through scattering with the medium, giving rise to secondary radiation which can be estimated by a factor which is called the "buildup factor." Manjunatha and Rudraswamy[1] studied energy absorption and exposure buildup factors in hydroxyapatite, and these are helpful in dosimetry and diagnostics. The same group[2,3] computed the buildup factors and photon relative dose distribution in different regions of teeth, which is useful in dental science. Previous researchers[4] also employed computed buildup factors for the estimation of specific absorbed fractions of energy in the biological samples. Previous researchers used exposure buildup factors for the calculations of secondary radiation dose such as bremsstrahlung[5,6]. Steel is used for shielding of gamma radiation.

Calculations of the energy absorbed in a medium include not only the contribution of uncollided photons from the source but also the contributions from the collided and secondary photons. In practice, this is done by multiplying the contribution of uncollided photons with the energy absorption buildup factor[7,8]. The buildup factor is an important parameter in the distribution of photon flux in every object. In brnchytherapy, radioactive seeds are implanted into the patient's body to destroy the cancerous tumor[9,10]. Thus, it is important to consider the photon buildup factor in the calculation of radiation dose received by the cancer cells. The buildup factor data were computed by different codes such as PALLAS-PL[11], RADHEAT-V4[12], ADJMOM-1[13] and ASFIT[14]. Several authors have provided different buildup factor data for extensive utilization of design in radiation shields and other purposes[15-19]. ANSI/ANS 6.4.3 used the geometric progression (GP) fitting method[20] and provided buildup factor data for 23 elements, water, air, and concrete at 25 standard energies in the energy range 0.015–15 MeV with suitable interval up to the penetration depth of 40 mfp.

Previous studies[21] compared the computed buildup factors using the GP fitting method with the PALLAS code. Good agreement was observed for penetration depth up to 40 mfp. Shimizu *et al.*[22] compared the buildup factors obtained by three different methods (GP fitting, invariant embedding, and Monte Carlo method), and only small discrepancies were observed for low-Z elements up to 10 mfp. Singh *et al.*[23] studied the variation of energy absorption buildup factors with incident photon energy and penetration

*Corresponding author (E-mail: manjunathhc@rediffmail.com)

depth for some solvents. Sidhu *et al.*[24] computed the exposure buildup factors in biological samples and studied the variation of exposure buildup factors with incident photon energy and effective atomic number. Previous researchers[25] studied X-ray and gamma radiation shielding parameters in silicon alloys. Silicon appears as coarse polyhedral particles and its hardness goes on increasing with increase in the number of silicon particles[26]. The influence of the Si content in the alloys have better wear resistance and mechanical properties[27]. The alloys with Boron content are used for the neutron shielding purpose[28]. The alloys with Boron content are possess good mechanical properties[29]. In the present study, we have studied the energy absorption buildup factors of the silicon-boron alloys of different composition such as alloy A-Si0.95-B0.05, alloy B- Si0.9-B0.1, alloy C- Si0.8-B0.2, alloy D- Si0.7-B0.3, alloy E- Si0.6-B0.4 and alloy F- Si0.5-B0.5 for wide energy range (0.015–15 MeV) up to the penetration depth of 40 mfp using GP fitting method. The consideration of the primary photons interaction in the target medium is not sufficiently accurate for the estimation of absorbed dose in other various organs from a source of photons. An accurate absorbed dose calculation needs specific absorbed fraction of energy (U). It is defined as the ratio of the energy absorbed by the target to the energy emitted by the source. In the present work, we have also studied the specific absorbed fraction of energy for the silicon-boron alloys of different composition such as alloy A-$Si_{0.95}$-$B_{0.05}$, alloy B- $Si_{0.9}$-$B_{0.1}$, alloy C- $Si_{0.8}$-$B_{0.2}$, alloy D- $Si_{0.7}$-$B_{0.3}$, alloy E- $Si_{0.6}$-$B_{0.4}$ and alloy F- $Si_{0.5}$-$B_{0.5.}$ for wide energy range (0.015–15 MeV) up to the penetration depth of 40 mfp.

2 Theory

Three methods are used to calculate the specific absorbed fraction of energy for a given source organ target organ pair at a given initial photon energy: (i) φ is calculated from the target to source to with the Monte Carlo radiation transport computer program; (ii) φ is calculated from source to target with the Monte Carlo computer program and this value is used to estimate target to source and (iii) φ is calculated from the target to source with the point source kernel method. In this method, the specific absorbed fraction of energy at distance x from the point source mono energetic photon emitter is given by:

$$\Phi(x)=\frac{\mu_{en}\exp(-\mu x)B_{en}}{4\pi R^2\rho} \quad \ldots (1)$$

Here, μ_{en} is linear absorption coefficient of photons of given energy, μ is linear attenuation coefficient of photons of given energy, B_{en} is energy absorption build up factor; ρ is density of the medium. The energy absorption build up factors are computed and are used to evaluate ϕ for the distance up to 10 mm and penetration depth up to 40 mean free paths.

In the present work, we have estimated energy absorption build up factor (B_{en}) using GP fitting method[30-37]. We have evaluated the G-P fitting parameters (b, c, a, X_k and d) for different alloys using following expression which is based on Lagrange's interpolation technique

$$P_{Z_{eff}}=\sum\left(\frac{\prod_{Z'\neq Z}(Z_{eff}-Z)}{\prod_{z\neq Z}(z-Z)}\right)P_z \quad \ldots (2)$$

where lower case z is the atomic number of the element of known G-P fitting parameter P_z adjacent to the effective atomic number (Z_{eff}) of the given material whose G-P fitting parameter $P_{Z_{eff}}$ is desired and upper case Z are atomic numbers of other elements of known G-P fitting parameter adjacent to Z_{eff}. For the computation of Z_{eff}, the values of mass attenuation coefficients were computed from WinXCom computer program[30]. Z_{eff} is computed from the following equations:

$$Z_{eff}=\frac{\frac{1}{N}\left(\frac{\mu}{\rho}\right)\sum n_iA_i}{\sum n_i}\Bigg/\frac{1}{N}\sum\left(\frac{f_iA_i}{Z_i}\right)\left(\frac{\mu}{\rho}\right) \quad \ldots (3)$$

Where n_i is the number of atoms of i^{th} element in a given molecule, (μ/ρ) is the mass attenuation coefficient of silicon-boron alloys, N is the Avogadro's number, A_i is the atomic weight of element i. $(\mu/\rho)_{st}$ was estimated based on the chemical composition and f_i is the fractional abundance.

GP fitting parameters (b, c, a, X_k and d) for element adjacent to Z_{eff} are provided by the standard data available in literature[37]. The computed G-P

fitting parameters (b, c ,a, X_k and d) were then used to compute the EABF in the energy range 0.015MeV-15MeV up to a penetration depth of 40 mean free path with the help of G-P fitting formula, as given by the equations[30-37]:

$$B(E,X) = 1 + \frac{b-1}{K-1}(K^X - 1) \text{ ; for K}\neq 1 \quad \ldots (4)$$

$$B(E,X) = 1 + (b-1)X \text{ ; for K=1} \quad \ldots (5)$$

$$K(E,X) = CX^a + d\frac{\tanh(\frac{X}{X_K} - 2) - \tanh(-2)}{1 - \tanh(-2)} \text{ ;}$$

For penetration depth (X)≤40mfp ... (6)

Where X is the source-detector distance for the medium in mean free paths (mfp) and b is the value of build-up factor at 1mfp. K(E,X) is the dose multiplication factor and b, c ,a, X_k and d are computed G-P fitting parameters that depend on attenuating medium and source energy.

3 Results and Discussion

We have calculated energy absorption buildup factors using GP fitting method. The calculated energy absorption buildup factors are graphically represented. The variation of energy absorption buildup factors with incident photon energy for silicon-boron alloys is shown in Fig. 1. From this figure, it is observed that energy absorption increases up to the E_{pe} (0.1 MeV) and then decreases. Here, E_{pe} is the energy value at which the photoelectric interaction coefficients match with Compton interaction coefficients for a given value of effective atomic number (Z_{eff}). The variation of buildup factors with energy is due to the dominance of photoelectric absorption in the lower end and the dominance of pair production in the higher photon energy region. As the energy of incident photon increases, Compton scattering overtakes the photoelectric absorption. It results in multiple Compton scattering events, which increases the energy absorption buildup factor up to the E_{pe}, and it becomes maximum at E_{pe}. Thereafter (above E_{pe}), pair production starts dominating (absorption process) which reduces the energy absorption buildup factor to a minimum value. The variation of energy absorption buildup factors with the penetration depth at 0.1 MeV, 1 MeV, 5 MeV, 10 MeV and 15 MeV is shown in Fig. 2. The buildup factor increases with the penetration depth.

The variation of specific absorbed fractions (φ) as a function of energy for silicon boron alloys are as shown in Fig. 3. It is observed that specific absorbed fractions increases up to the E_{pe} and then decreases. Here E_{pe} is the energy value at which the photo electric interaction coefficients matches with Compton interaction coefficients for a given value of effective atomic number (Z_{eff}). The variation of specific absorbed fractions with mean free path at various energies (0.05, 0.1, 0.5, 1.0, 5.0, 10 and 15 MeV) for different silicon boron alloys are as shown in Fig. 4. From this Figure it is clear that specific absorbed fractions value increases with

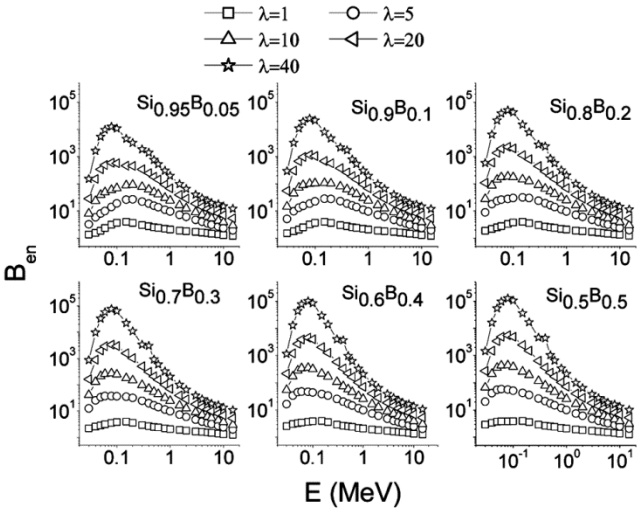

Fig. 1 – Variation of buildup factors (Ben) of different silicon-boron alloys with energy (MeV) for different mean free paths (Alloy A-$Si_{0.95}$-$B_{0.05}$, Alloy B- $Si_{0.9}$-$B_{0.1}$, Alloy C- $Si_{0.8}$-$B_{0.2}$, Alloy D- $Si_{0.7}$-$B_{0.3}$, Alloy E- $Si_{0.6}$-$B_{0.4}$ and Alloy F- $Si_{0.5}$-$B_{0.5}$.)

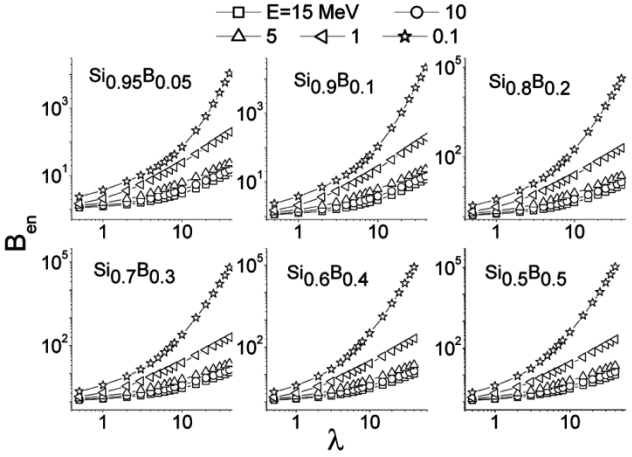

Fig. 2 – Variation of buildup factors (Ben) of different silicon-boron alloys with mean free path at different energies (MeV). (Alloy A-$Si_{0.95}$-$B_{0.05}$, Alloy B- $Si_{0.9}$-$B_{0.1}$, Alloy C- $Si_{0.8}$-$B_{0.2}$, Alloy D- $Si_{0.7}$-$B_{0.3}$, Alloy E- $Si_{0.6}$-$B_{0.4}$ and Alloy F- $Si_{0.5}$-$B_{0.5}$.)

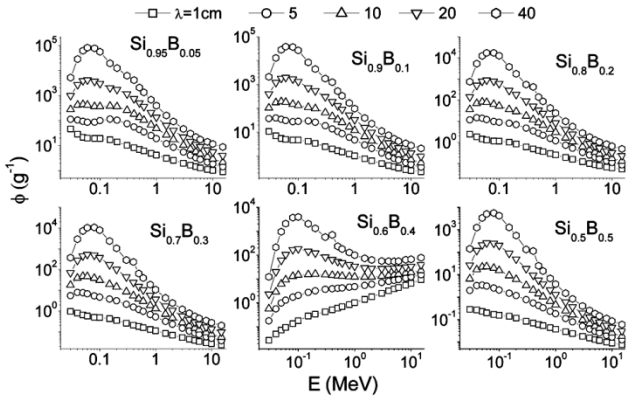

Fig. 3 – Variation of specific absorbed fractions (φ) (g^{-1}) as a function of energy (MeV). (Alloy A-$Si_{0.95}$-$B_{0.05}$, Alloy B- $Si_{0.9}$-$B_{0.1}$, Alloy C- $Si_{0.8}$-$B_{0.2}$, Alloy D- $Si_{0.7}$-$B_{0.3}$, Alloy E- $Si_{0.6}$-$B_{0.4}$ and Alloy F- $Si_{0.5}$-$B_{0.5.}$)

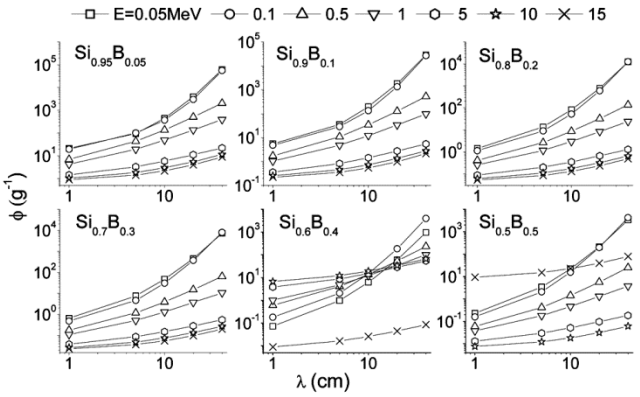

Fig. 4 – Variation of specific absorbed fractions (φ) (g^{-1}) as a function of mean free path (λ). (Alloy A-$Si_{0.95}$-$B_{0.05}$, Alloy B- $Si_{0.9}$-$B_{0.1}$, Alloy C- $Si_{0.8}$-$B_{0.2}$, Alloy D- $Si_{0.7}$-$B_{0.3}$, Alloy E- $Si_{0.6}$-$B_{0.4}$ and Alloy F- $Si_{0.5}$-$B_{0.5.}$)

increase in the target distance. This is due to the reason that with increase in the target distance, scattering events in the medium increases.

Variation of effective electron density and specific absorbed fractions (φ) as a function effective atomic number for silicon boron alloys are as shown in Figs 5 and 6. The effective electron density and specific absorbed fractions for boron polymers is large in the low energy region (due to photo electric effect) and decreases progressively, there after increases and becomes constant for high energy (due to pair production). Figure 7 shows the comparison of specific absorbed fraction of energy among the studied silicon boron alloys at different energies for mean free paths corresponding to 20 and 40. From this comparison, it is clear that the silicon boron alloy $Si_{0.95}$-$B_{0.05}$ is having larger value of specific absorbed fractions than the other studied alloys.

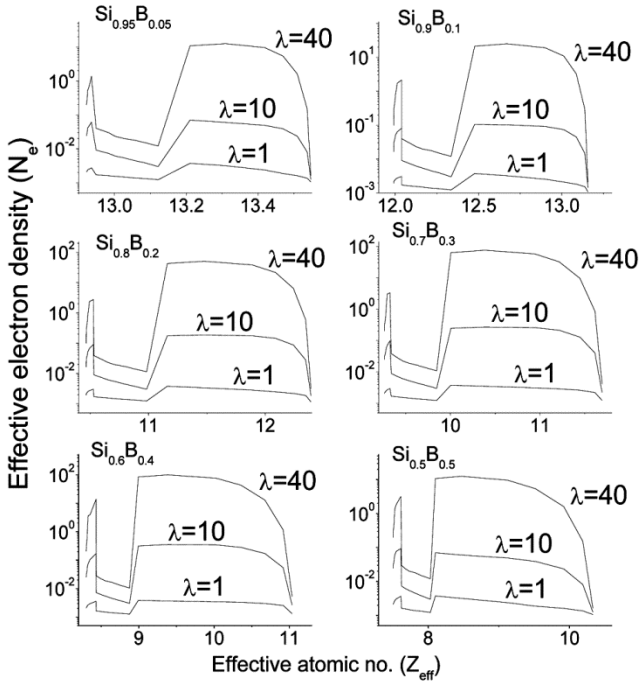

Fig. 5 – Variation of effective electron density as a function of effective atomic number. (Alloy A-$Si_{0.95}$-$B_{0.05}$, Alloy B- $Si_{0.9}$-$B_{0.1}$, Alloy C- $Si_{0.8}$-$B_{0.2}$, Alloy D- $Si_{0.7}$-$B_{0.3}$, Alloy E- $Si_{0.6}$-$B_{0.4}$ and Alloy F- $Si_{0.5}$-$B_{0.5.}$)

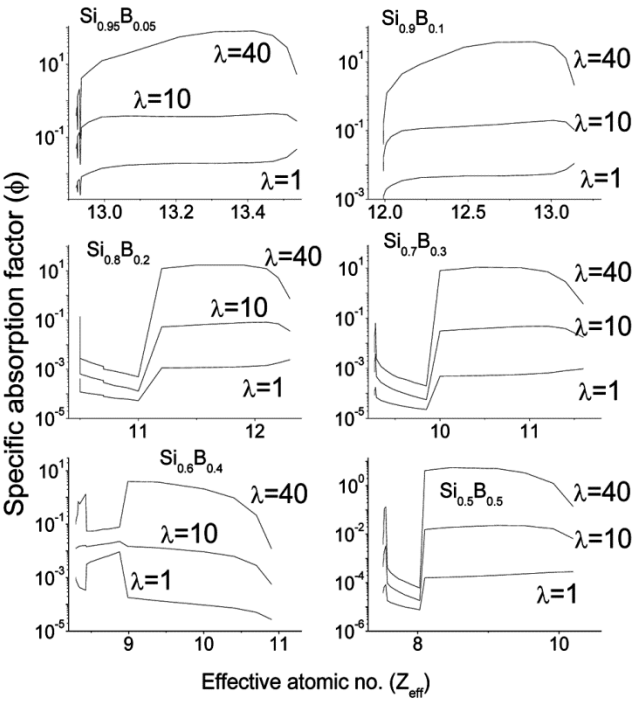

Fig. 6 – Variation of specific absorption factor as a function of effective atomic number. (Alloy A-$Si_{0.95}$-$B_{0.05}$, Alloy B- $Si_{0.9}$-$B_{0.1}$, Alloy C- $Si_{0.8}$-$B_{0.2}$, Alloy D- $Si_{0.7}$-$B_{0.3}$, Alloy E- $Si_{0.6}$-$B_{0.4}$ and Alloy F- $Si_{0.5}$-$B_{0.5.}$)

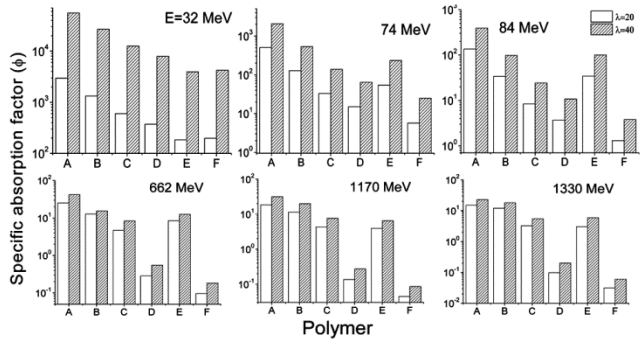

Fig.7 – Comparison of specific absorption factor with silicon-boron alloys at different energies for mean free path corresponding to 20 and 40. (Alloy A-$Si_{0.95}$-$B_{0.05}$, Alloy B- $Si_{0.9}$-$B_{0.1}$, Alloy C- $Si_{0.8}$-$B_{0.2}$, Alloy D- $Si_{0.7}$-$B_{0.3}$, Alloy E- $Si_{0.6}$-$B_{0.4}$ and Alloy F- $Si_{0.5}$-$B_{0.5.}$).

4 Conclusions

We have studied the energy absorption buildup factors and specific absorbed fraction of energy for the silicon-boron alloys of different composition. From this study, we can suggest that the silicon boron alloy $Si_{0.95}$-$B_{0.05}$ is the good absorber of X-ray, gamma and it can be used for shielding purpose.

References

1 Manjunatha H C & Rudraswamy B, *Radiat Meas*, 47 (2012) 364.
2 Manjunatha H C & Rudraswamy B, *Radiat Phys Chem*, 80 (2011) 14.
3 Manjunatha H C & Rudraswamy B, *J Radio Nucl Chem*, 294 (2012) 251.
4 Manjunatha H C & Rudraswamy B, *Ann Nucl Energy*, 38 (2011) 2271.
5 Manjunatha H C, *Appl Rad Isotopes*, 94 (2014) 282.
6 Manjunatha H C & Rudraswamy B, *Phys Med*, 27 (2011) 188.
7 Harima Y, Nucl Sci Eng, 83 (1983) 299.
8 Shultis J K & Faw R E, *Health Phys*, 88 (2005) 587.
9 Chibani O, *Med Phys*, 32 (2005) 3688.
10 Tsiakalos M F, *Radio Ther Oncol*, 79 (2006) 131.
11 Takeuchi K & Pallas-Pl S P, *Ship Res Inst*, 42 (1973).
12 Yamano N, Minami K, Koyama K & Naito Y, *Atom Energy Res Inst Rep Jpn*, 1316 (1989).
13 Simmons G L, National Bureau of Standards Technical Note, (1973) 748.
14 Gopinath D V & Samthanam K, *Nucl Sci Eng*, 43 (1971) 186.
15 Hubbell J H, *J Res*, 67C (1963) 291.
16 Chilton A B, Eisenhauer C M & Simmons G L, Nucl Sci Eng, 73 (1980) 97.
17 Sakamoto Y, Tanaka S & Harima Y, *Nucl Sci Eng*, 100 (1988) 33.
18 Brar G S, Sandhu A K, Makhan S & Mudahar G S, *Radiat Phys Chem*, 44 (1994) 459.
19 Brar G S & Mudahar G S, *Nucl Geophys*, 9 (1995) 471.
20 American National Standard (ANS). (1991).
21 Harima Y, Sakamoto Y, Tanaka S & Kawai M, *Nucl Sci Eng*, 94 (1986) 24.
22 Shimizu A, Onda T & Sakamoto Y, *J Nucl Sci Technol*, 41 (2004) 413.
23 Singh P S, Tejbir S & Paramajeet K, *Ann Nucl Energy*, 35 (2008) 1093.
24 Sidhu G S, Singh P S & Mudahar G S, *J Radiol Prot*, 20 (2000) 53.
25 Manjunatha H C, Sathish K V & Seenappa L, *Radiat Phys Chem*, 165 (2019) 108414.
26 Torabian H, Pathak J P & Tiwari S N, *Wear*, 177 (1994) 47.
27 Singh M, Prasad B K, Mondal D P & Jha A K, *Tribol Int*, 34 (2001) 557.
28 Nakaidze, Gharibashvili, Antadze M & Tsagareishvili, *J Solid State Chem*, 177 (2004) 592.
29 Zhang S, Song J, Liao H & Liu Y, *Materials*, 12 (2019) 1100.
30 Leif G, Guilbert N, Jensen K B & Leving H, *Radiat Phys Chem*, 71 (2004) 653.
31 Manjunatha H C & Rudraswamy B, *Radiat Meas*, 47 (2012) 364.
32 Manjunatha H C & Rudraswamy B, *Radiat Phys Chem*, 80 (2011) 14.
33 Manjunatha H C & Rudraswamy B, *J Radio Nucl Chem*, 294 (2012) 251.
34 Manjunatha H C & Rudraswamy B, *Health Phys*, 104 (2013) 158.
35 Suresh K C, Manjunatha H C & Rudraswamy B, *Radiat Prot Dosimetry*, 128 (2007) 294.
36 Manjunatha H C & Rudraswamy B, *Health Phys*, 100 (2011) S92.
37 Manjunatha H C, *J Med Phys*, 39 (2014) 112.
38 American National Standard, ANSI/ANS 6.4.3. Oak Ridge, TN 37831-6362 (1991).